

# Quenched $SU(3)$ hadron spectroscopy using improved fermionic and gauge actions

Sara Collins, Robert G. Edwards\*, Urs M. Heller, and John Sloan  
 SCRI, Florida State University, Tallahassee, FL 32306-4052, USA

We present results of quenched  $SU(3)$  hadron spectroscopy using  $\mathcal{O}(a)$  improved Wilson fermions. The configurations were generated using an  $\mathcal{O}(a^2)$  improved 6-link  $SU(3)$  pure gauge action at  $\beta$ 's corresponding to lattice spacings of 0.43, 0.25, 0.20, 0.18, and 0.15 fm. We find evidence that fermionic scaling violations are consistent with  $\mathcal{O}(a^2)$  errors.

## 1. INTRODUCTION

The Symanzik action improvement program has been proposed [1,2] as a way to reduce scaling violations in the approach to the continuum limit from a lattice action. In another contribution, we report on our preliminary investigations into the nature of scaling violations inherent in improved actions. In another proceedings in this volume[4], we make detailed comparisons of Wilson and tadpole-improved Clover fermion actions on configurations with dynamical fermion content. In this work, we perform  $SU(3)$  quenched spectroscopy using a one-loop tadpole-improved Symanzik pure gauge action and the tree-level tadpole-improved Clover fermion action. We measure the hadron spectrum and the string tension at lattice spacings 0.15, 0.18, 0.20, 0.25, and 0.43 fm. The goal of this work is to measure the lattice spacing dependence of the hadron spectrum. We find significant scaling violations in  $am_{K^*}/\sqrt{a^2\sigma}$  consistent with  $\mathcal{O}(a^2)$ .

## 2. ACTIONS

Recently, it was shown [3] that the tadpole improved Symanzik inspired pure gauge action [1] is successful in restoring Lorentz invariance in the static quark potential even at a lattice spacing of 0.43fm. Inspired by this result, we used the action

$$S[U] = \beta_{\text{pl}} \left[ \sum_{\text{pl}} \frac{1}{3} \text{Re Tr } U_{\text{pl}} + c_{\text{rt}} \sum_{\text{rt}} \frac{1}{3} \text{Re Tr } U_{\text{rt}} \right. \quad (1)$$

$$\left. + c_{\text{pg}} \sum_{\text{pg}} \frac{1}{3} \text{Re Tr } U_{\text{pg}} \right], \quad (1)$$

where

$$c_{\text{rt}} = -(1 + 0.4805\alpha_s) / 20u_0^2 \quad (2)$$

$$c_{\text{pg}} = -0.03325\alpha_s / u_0^2 \quad (3)$$

The sums are over plaquettes (pl),  $1 \times 2$  rectangles (rt), and the six length path  $(\mu, \nu, \rho, -\mu, -\nu, -\rho)$  with  $\mu, \nu, \rho$  all different (pg). We use the measured expectation value of the plaquette to determine  $u_0$ . The coupling constant  $\alpha_s$  is calculated using the tree level action,

$$u_0 = \left( \frac{1}{3} \text{Re Tr } \langle U_{\text{pl}} \rangle \right)^{1/4} \quad (4)$$

$$\alpha_s = -\frac{\log \left( \frac{1}{3} \text{Re Tr } \langle U_{\text{pl}} \rangle \right)}{3.06839} \quad (5)$$

Classically, this action has  $\mathcal{O}(a^4)$  errors but quantum effects induce  $\mathcal{O}(a^2 a^2)$  errors. However, it was shown [3] that the action (1) is insensitive to nonperturbative tuning of the coefficients suggesting that the  $\mathcal{O}(a^2 a^2)$  errors are small.

To reduce fermionic scaling errors, we use the tadpole-improved version of the tree-level Clover fermionic action proposed in [2].

$$S_F^{SW} = S_F^W - ic(g_0^2) \frac{\kappa}{2u_0^3} \sum_{x, \text{pl}} \bar{\psi}(x) \sigma_{\text{pl}} F_{\text{pl}}(x) \psi(x), \quad (6)$$

where  $S_F^W$  is the usual Wilson fermionic action and  $F_{\text{pl}}$  is a lattice definition of the field strength tensor. For the tree level action,  $c(g_0^2) = 1$ .

\*Speaker at the conference

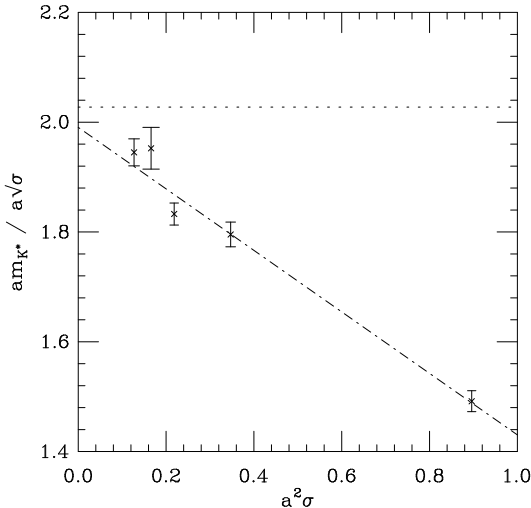


Figure 1. Scaling plot of  $am_{K^*}$  versus the string tension  $a^2\sigma$ . The horizontal line is the physical value using  $a^2\sigma = 440\text{MeV}$ . The diagonal line is a least squares fit.

With this tree-level action, one expects quantum errors of  $\mathcal{O}(\alpha a)$ . However, Naik [5] computed the one loop and the dominant two loop contributions to  $c(g_0^2)$  and finds that after tadpole improvement the coefficient of  $g_0^2$  is 0.016. Therefore, we expect to see only the dominant  $\mathcal{O}(a^2)$  fermionic errors.

### 3. OBSERVABLES

To set the scale,  $a$ , we used the string tension. We computed finite  $T$  approximations to the static quark potential using time-like Wilson loops  $W(\vec{R}, T)$  which were constructed using ‘APE’-smeared spatial links [6]. On and off-axis spatial paths were used with distances  $R = n, \sqrt{2n}, \sqrt{3n}$  and  $\sqrt{5n}$ , where  $n$  is a positive integer. The “effective” potentials were fitted using a correlated  $\chi^2$  procedure with the spatial covariance estimated using bootstrap. The string tension was estimated using the form

$$V(\vec{R}) = V_0 + \sigma R - \frac{e}{R} - f \left( G_L(\vec{R}) - \frac{1}{R} \right). \quad (7)$$

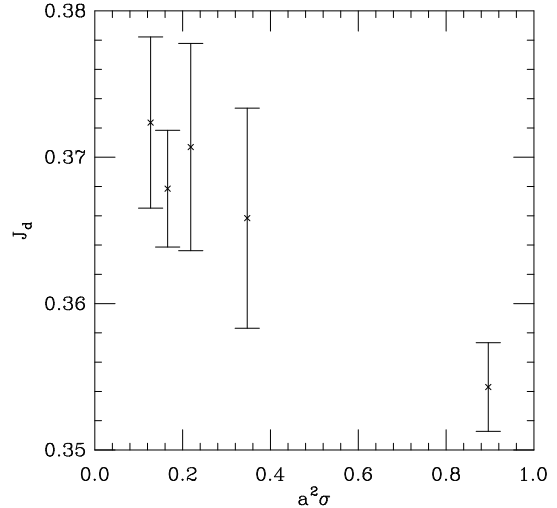


Figure 2. Scaling plot of  $J_d$  versus the string tension  $a^2\sigma$ . The physical value is 0.499.

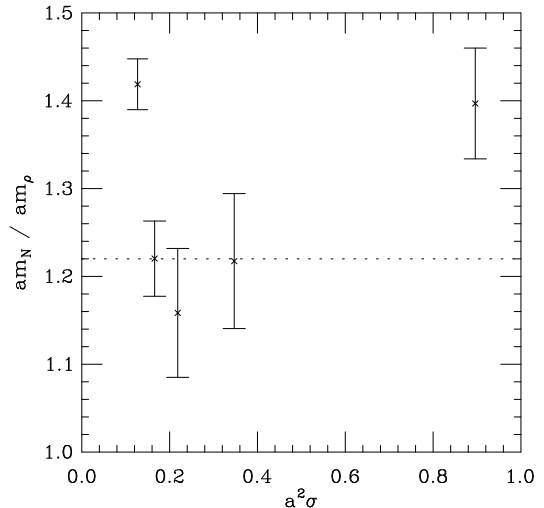


Figure 3. Scaling plot of the nucleon versus the rho as a function of the string tension  $a^2\sigma$ . The horizontal line is the physical value of 1.22.

The last term takes account of the lattice artifacts at short distance. Here,  $G_L(\vec{R})$  denotes the lattice Coulomb potential for the Wilson gluonic propagator. We did not have available the lattice Coulomb potential for the tree-level Symanzik action; however, we found  $G_L(\vec{R})$  enabled fits to smaller  $R$ .

For hadron measurements, we used correlated multi-state fits to multiple correlation functions as discussed in [4]. We computed quark propagators in Coulomb gauge at four  $\kappa$  values for each  $\beta$ . We used two gaussian source smearing functions with smeared and local sinks. The widths were chosen to have a positive and negative overlap, respectively, with the first excited state. This improved the signal for the excited state in a multi-state (“vector”) fit. We also measured mixed valence content mesons and baryons.

As discussed in [4], we tried to avoid human intervention as much as possible in the fitting procedure. For the multistate fits, we chose the plateau with  $\max N_{dof} Q \prod_i \delta M_i / M_i$  where the product is over the relative errors of the ground and first excited state masses, and  $Q$  is the confidence level for a  $N_{dof}$  degree of freedom fit.

Once a fitting range was chosen, a bootstrap ensemble of masses was generated and used for correlated  $\chi^2$  chiral fits. We fit the particle mass according to the ansätze

$$M_{\text{particle}} = \begin{cases} C_0 + C_2 M_{PS}^2 \\ C_0 + C_2 M_{PS}^2 + C_3 M_{PS}^3 \end{cases} \quad (8)$$

This ansatz was motivated by one loop chiral perturbation corrections to baryon masses. We note that recently one loop  $M_{PS}^3$  corrections to the vector mass were derived in [7].

An important method used to increase statistics is via ‘ $Z(3)$ ’ fermion sources [8]. Within the source time-slice source for quark propagators, smearing functions are placed at regular intervals along each spatial dimension. These smearing functions are weighted with random elements chosen according to a  $Z(3)$  distribution. Since the elements are not correlated, each origin in a mesonic or baryonic construction contribute independently to the correlation functions. The distance between origins should be chosen larger than the lattice size of a physical state or the

smearing width used.

#### 4. SIMULATIONS

We generated quenched configurations using the action (1) at  $\beta = 7.90, 7.75, 7.60, 7.40$ , and  $6.80$ . Unfortunately, the non-local nature of the action precluded an efficient implementation of an over-relaxed / heat-bath algorithm for the CM-2 at SCRI – we would need to divide the lattice into 32 sublattices. We used a Hybrid Monte Carlo algorithm with a second order integration scheme, step size  $\delta = 0.1$ , and a global acceptance test. We typically found  $> 0.75\%$  acceptance rates.

We determined meson and baryon masses using the action (6). The pseudoscalar masses were tuned to the same physical mass (in units of  $\sqrt{a^2\sigma}$ ) between the various  $\beta$ . The vector to pseudoscalar mass ratios varied from about 2.0 down to 1.2. At the coarsest lattice, we found a large number of exceptional configurations on an  $8^3 \times 16$  lattice. To avoid problems, we used a  $16^3 \times 32$  lattice throughout except at  $\beta = 7.40$ . We expect finite volume effects to be small since the box size is 2.40fm at  $\beta = 7.90$ .

The results of the chiral extrapolations of our best fits are listed in Table 1 along with the string tension. Note the lattices are too coarse to reliably use Sommer’s force method since the lattice spacing is close to the empirical 0.5fm scale. The lattice spacings we quote used  $\sqrt{a^2\sigma} = 440\text{MeV}$ . For the vector mesons, we used a quadratic fit ansatz of (8) for  $\beta = 7.90, 7.75$ , and  $7.60$  using all 10 mixed valence states. At  $\beta = 7.40$ , we dropped the two largest masses and used a for a quadratic fit.

At  $\beta = 6.80$ , we found some interesting results. First, the assumption of using mixed valence states as distinct measurements appeared to break down – the meson masses fluctuated significantly enough to lower the quality of the fit. For this reason, we only used the four diagonal masses (same valence content) for fits. Also, the smallest pseudoscalar measured had  $am_{PS} = 0.9939(13)$ . At these large masses, we expect significant deviations from the continuum dispersion relations. Quite significantly, a quadratic fit ansatz was clearly violated, and we used a cubic fit ansatz

Table 1

String tension and best fits of masses extrapolated to physical ratios.

$\beta$	$L$	$N_{meas}$	$u_0$	$a^2\sigma$	$am_\rho$	$am_{K^*}$	$J_d$	$am_N$
7.90	16	100	0.8848	0.1272( 16)	0.6206( 58)	0.6937(44)	0.3724(58)	0.881( 1)
7.75	16	100	0.8800	0.1658( 50)	0.7123( 46)	0.7950(35)	0.3679(40)	0.869(25)
7.60	16	32	0.8736	0.2184( 13)	0.7666( 85)	0.8565(68)	0.3707(71)	0.888(46)
7.40	8	68	0.8629	0.3470( 29)	0.9482(115)	1.0577(89)	0.3658(75)	1.154(59)
6.80	16	72	0.8261	0.8961(177)	1.2706( 71)	1.4120(41)	0.3543(30)	1.778(70)

of (8) with  $N_{dof} = 1$ . This indicates that scaling violations inherent with large  $am_q$  are roughly approximated by higher order terms in the chiral ansatz of (8).

In our chiral fits for the nucleon, we only used the four diagonal masses. For all propagator fits, we used a two exponential fit with two smearings. At  $\beta = 7.90 - 7.40$ , we found that the quadratic ansatz broke down at the largest mass. However, there was not sufficient signal for a cubic term. At  $\beta = 6.80$ , we used a cubic ansatz for all four masses. At  $\beta = 7.90$ , the extrapolated nucleon value is way off scaling. We think this comes from a lack of statistics due to autocorrelations, and the error bar is underestimated.

## 5. SCALING VIOLATIONS

Our main result for the determination of scaling violations is in Figure 1. We interpolate (or extrapolate) the vector meson mass to the  $K^*/K$  ratio and find that there are significant scaling violations in the  $am_{K^*}/\sqrt{a^2\sigma}$  ratio. Fitting to a line, we find  $Q = 0.1$  and the intercept of 1.99(2) which is close to the physical value of 2.03 using  $\sqrt{a^2\sigma} = 440\text{MeV}$ . This implies that the assumption of  $\mathcal{O}(a^2)$  errors is significant. If we fit to  $\sqrt{a^2\sigma}$  assuming  $\mathcal{O}(a)$  errors, we find that  $Q = 0.17$  but the intercept is 2.22(3). This value would imply  $\sqrt{a^2\sigma} = 347\text{MeV}$  which is probably too low. Indeed, constraining the  $\mathcal{O}(a)$  fit to pass through the value 2.0275 has  $Q = 10^{-9}$ . We thus feel reasonably confident that the fermionic scaling errors are (at least) consistent with  $\mathcal{O}(a^2)$ .

Following [9], we plot the ratio

$$J_d = am_{K^*} \frac{am_{K^*} - am_\rho}{(am_K)^2 - (am_\pi)^2} \quad (9)$$

versus  $a^2\sigma$  in Figure 2. We see that  $J_d$  is reasonably scaling out to  $\beta = 7.40$  indicating that scaling violations in the individual masses are nearly canceling in the ratio. The value of  $J_d$  is consistent with other quenched calculations.

In Figure 3, we plot the ratio of  $am_N/am_\rho$ . We see reasonable scaling out to  $\beta = 7.40$ , but the value at  $\beta = 7.90$  is way off as described above.

The computations done on the CM-2 at S.C.R.I. This research was supported by DOE contracts DE-FG05-85ER250000 and DE-FG05-92ER40742.

## REFERENCES

1. See M. Lüscher and P. Weisz, Phys. Lett. **158B**, 250(1985), and references therein.
2. B. Sheikholeslami and R. Wohlert, Nucl. Phys. **B259**, (1985) 572.
3. M. Alford *et al.*, Nucl. Phys. B (Proc. Suppl.) **42** (1995) 787; FERMILAB-Pub 95/199-T, hep-lat/9507010.
4. S. Collins, R.G. Edwards, U.M. Heller, and J. Sloan, Proceedings of the Lattice '95 conference (Melbourne, Australia, July 1995), to appear in Nucl. Phys. B (Proc. Suppl.).
5. S. Naik, Phys. Lett. **B311** (1993) 230.
6. M. Albanese *et al.* (APE Collaboration), Phys. Lett. **B192** (1987) 163.
7. E. Jenkins *et al.*, UCSD-PTH-95-08 (1995), hep-ph/9506356.
8. F. Butler *et al.*, Nucl. Phys. **B421**, (1994) 217, and references therein.
9. P. Lacock and C. Michael, LTH-349, hep-lat/9506009.